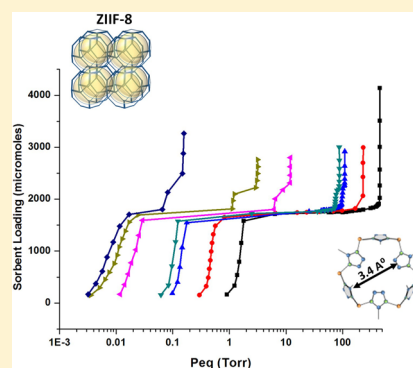


Evidence of Gate-Opening on Xenon Adsorption on ZIF-8: An Adsorption and Computer Simulation Study

Dinuka H. Gallaba,[†] Alberto G. Albesa,[‡] and Aldo D. Migone^{*,†}[†]Department of Physics, Southern Illinois University, Carbondale, Illinois 62901, United States[‡]Departamento de Química, Universidad Nacional de La Plata, 47 y 115, La Plata, Argentina and Researcher at the Instituto Nacional de Investigaciones Fisicoquímicas Teóricas y Aplicadas (INIFTA-CONICET) Diagonal 113 entre 63 y 64, La Plata, Argentina

Supporting Information

ABSTRACT: We report on experimental (thermodynamics and kinetics) and computer simulation results for Xe sorption in ZIF-8. At temperatures below ~ 145 K, there are two substeps present in adsorption isotherms (before saturation is reached). The substep that occurs at higher loadings was identified as corresponding to ZIF-8's gate-opening transition. Above 145 K, this higher-loading substep is no longer resolvable. We determined the isosteric heat of adsorption for this system and obtained a value of 244 meV for sorption on the more strongly binding sites in the ZIF-8. We found that there is a peak in the isosteric heat of adsorption, as a function of sorbent loading, associated with the gate-opening transition. We estimated the heat of transition for gate-opening to have an upper bound of ~ 30 meV. Our results for the isotherms and the isosteric heats are compared with those from our Monte Carlo computer simulations, obtained using both the structure of ZIF-8 before and after the gate-opening transition and a new set of mixed Lennard-Jones parameters. We conducted measurements for the sorption kinetics for this system. We found that, while the sorption occurs faster as the loading increases before the gate-opening transition, the equilibration times increase with loading in the gate-opening region, resulting in an unusual nonmonotonic behavior for the variation of this quantity as a function of sorbent loading.



1. INTRODUCTION

Adsorption plays a central role in the study of porous materials. On one hand, it provides a fundamental tool for their characterization and allows us to gain a degree of understanding of their behavior. On the other hand, it is the basic process through which some very useful practical applications of porous materials are achieved. It has been noted that the discovery or synthesis of new classes of porous materials is associated with the expansion and renewal of technological applications of sorption processes.¹ It is also true that the development or discovery of new types of porous sorbents has often led to basic studies of new physical behavior in systems formed by sorbates interacting with sorbents.^{2,3}

One of the most important classes of porous materials produced in recent times are porous metal–organic frameworks (MOFs).^{4–7} Porous MOFs are a group of microporous materials (the term is used here to indicate materials with pore sizes smaller than 2 nm, in accordance with the classification recommended by IUPAC for porous materials,⁸ although a perhaps more descriptive term would be nanoporous) that contains metal oxide or nitride clusters connected by organic linkers. By properly combining different basic assembly units, MOFs of a variety of geometries, effective specific surface areas, pore volumes, and pore diameters have been synthesized.^{4,5}

There is a subgroup among the MOFs called ZIFs (for zeolitic imidazolate frameworks) which consists of tetrahedral

metals (Zn, In, Mo) linked by imidazolate ($C_4H_3N_2$) units.^{9–11} ZIFs have structures that are closely related to those of zeolites. From the perspective of practical applications, ZIFs offer the advantage over most other MOFs of having a much higher degree of both thermal and chemical stability.¹⁰ In addition, some ZIFs are commercially available.¹² Commercially available MOFs are generally much less expensive than other types of novel porous materials (such as carbon nanotubes or carbon nanohorns).¹²

ZIF-8 is of the most extensively studied materials among the ZIFs.¹³ In ZIF-8, the imidazolate (IM) unit makes a metal–IM–metal angle which closely matches that of the Si–O–Si angle in zeolites; it is the structural analogue of sodalite.¹⁰

ZIF-8 consists of relatively large cages, of approximately 11.4 Å in diameter, each connected to eight neighboring cavities through six-membered ring windows, of approximately 3.4 Å diameter¹⁴ (Figure 1).

As is the case for many zeolites, ZIF-8 is a flexible structure.¹⁵ ZIF-8's flexibility has been demonstrated by the sorption of a number of species larger than the size of the windows present in its structure.^{14,16–18} For example, xenon's atomic diameter is ~ 4.4 Å; consequently, it is not able to penetrate rigid windows of 3.4 Å in diameter. However, as we report below, xenon

Received: April 5, 2016

Revised: June 1, 2016

Published: June 30, 2016

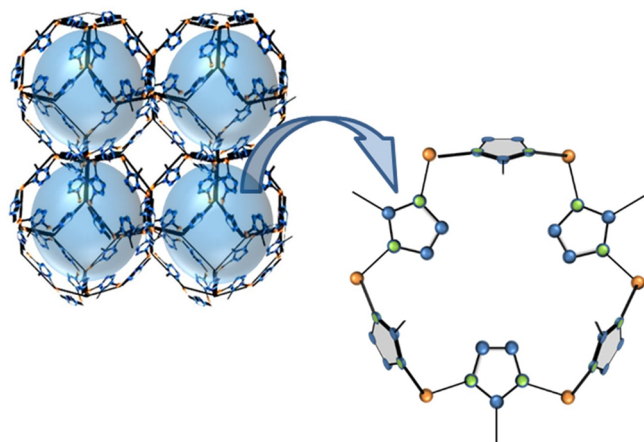


Figure 1. ZIF-8 window of the cavity structure: pentagons are the imidazolate ($C_4H_3N_2$) linkers, and orange spheres are the Zn atoms.

readily sorbs in ZIF-8, confirming the flexible nature of the structure of this material.

While the often implicit assumption that the sorbent remains unaltered during adsorption is generally made in sorption studies, such an assumption is not valid for ZIF-8. This is because, in some cases, ZIF-8 undergoes a structural transition upon sorption: gate-opening. This transition was first identified in high-pressure experiments (the transition occurred at pressures on the order of 1.4 GPa at room temperature).¹⁹ In gate-opening, the imidazolate linkers of ZIF-8 reorient to increase the window size of the structure. Gate-opening has been observed to occur as a result of the sorption of some gases, including Ar, O₂, N₂, and CO, at pressures below 1 atm at cryogenic temperatures.^{14,16–18} In these cases, the structural transition is reflected in the adsorption data by the presence of substeps in the isotherms (i.e., regions of very steep increase in loading at nearly constant pressure, which appear for different values of the pressure as sorbent loading increases).^{14,16–18}

There have been few prior studies of Xe on ZIF-8. A temperature-programmed desorption study of Kr and Xe on several MOFs, including ZIF-8, found that the final desorption temperature for Xe (~ 190 K) was considerably higher than that for Kr (~ 145 K). This behavior is the one expected when Xe has stronger sorbent–sorbate interactions with ZIF-8 than Kr, and both are sorbing in it, so this study provided the first experimental indication that Xe was able to sorb in ZIF-8.²⁰ A ¹²⁹Xe NMR study conducted at 1 and 10 Torr found that a chemical shift occurred in this system at temperatures between 150 and 170 K.²¹ The shift was taken as an indication of the reorientation of the organic linkers taking place in this temperature range.²¹ In this same study, partial adsorption isotherms measured between 173 and 273 K for pressures below 1100 Torr yielded isosteric heats of adsorption between 20 and 24 kJ/mol at higher loadings, with lower isosteric heats (between 15 and 20 kJ/mol) at lower loadings.²¹ In a patent application for the use of ZIF-8 for the differential adsorption of Xe over Kr or Ar, data were presented for the dependence of the isosteric heat of adsorption at 273 K for Xe adsorption on ZIF-8.²² The isosteric heat of adsorption started at approximately 20 kJ/mol at low loadings and increased slowly from this value as the loading increased.²² A very recent study reports on synchrotron X-ray measurements of Xe as a function of pressure along a 180 K isotherm. This study determined where the sorption sites are for Xe in ZIF-8, and what is the sequence

in which the sites are occupied.²³ It determined that, before the gate-opening transition, the most numerous sorption sites are close to the carbon double-bonds, on the imidazoles, and that there are also sites at the center of the six-ring windows, and sites at the center of the four-membered windows. The X-ray diffraction study found that there were four groups of binding sites for Xe on ZIF-8. After the gate-opening transition takes place (which they observe occurring at a pressure somewhere between 90 and 390 mbar in their 180 K data), the sites at the center of the four-membered Zn–N₄ windows become empty, and sites at the center of the pore become occupied.²³

Here we report the results of an adsorption study of Xe on ZIF-8 at temperatures between 95 and 160 K. Our results include equilibrium measurements as well as adsorption kinetics experiments, and the results of a Monte Carlo computer simulation study for this system. We determined the isosteric heat of adsorption as a function of sorbent loading from the isotherms. Our computer simulation results are compared with our equilibrium experimental results, as well as with results obtained in other computer simulation studies.^{14,24–26} Our equilibrium experimental work sheds light on the temperature dependence of the gate-opening transition for this system, presents evidence for the existence of a peak in the isosteric heat of adsorption (plotted as a function of loading) associated with the gate-opening transition, and allows the determination of an upper bound for the heat evolved in the gate-opening transition. Our kinetics results provide information on the dependence of the equilibration times on sorbent loading, and generally on the behavior of the kinetics of adsorption on this system.¹⁸

2. EXPERIMENTAL TECHNIQUES

The ZIF-8 sample that was used in these experiments was manufactured by BASF and sold by Sigma-Aldrich as “Basolite Z1200”.¹² The mass of the sample used in the measurements was 0.1858 g. The ZIF-8 sample was transferred, in air, to a stainless steel cell which was subsequently sealed with a copper gasket and connected to a vacuum pumping station. The cell was heated up to 120 °C and kept overnight under a vacuum (of 1×10^{-6} Torr) at this temperature. The ZIF-8 was not re-exposed to air after the heating under a vacuum was completed.

The experimental cell was connected to a helium closed-cycle refrigerator. The cell temperatures were controlled to better than ± 20 mK using an arrangement of two separate temperature controllers.

The gas used in the measurements was research grade Xe from Matheson. The adsorption setup is a specialty built automated unit. The adsorption measurements (gas dosing and recording of the pressures) are carried out using an in-house written program in Lab-View.¹⁸ It typically takes 2–3 weeks to complete one isotherm.

3. RESULTS

3.1. Isotherms. We determined the effective specific surface area of the ZIF-8 sample using the “point B” method. That is, we determined the total amount of Xe sorbed on the ZIF-8 up to the so-called “point B” in the isotherm, and then calculated the area that would be needed to adsorb that same amount of xenon as a monolayer.²⁷ The effective specific surface area of the ZIF-8 sample is 1278 m²/g (in reasonable agreement with previously determined values for this quantity).¹⁸

Our adsorption isotherm measurements span seven temperatures in the range between 95 and 160 K. All of the temperatures in this interval are below xenon's triple point ($T_t = 161.389$ K), so solid xenon is the phase that condenses at saturation in our measurements.²⁸ In all cases, the measurements were started from a freshly re-evacuated sample (i.e., from zero loading) and were continued, without re-evacuation, until the equilibrium pressure reached saturation.

Figure 2 presents a semilogarithmic plot of the adsorption data that summarizes many of our equilibrium results. The data

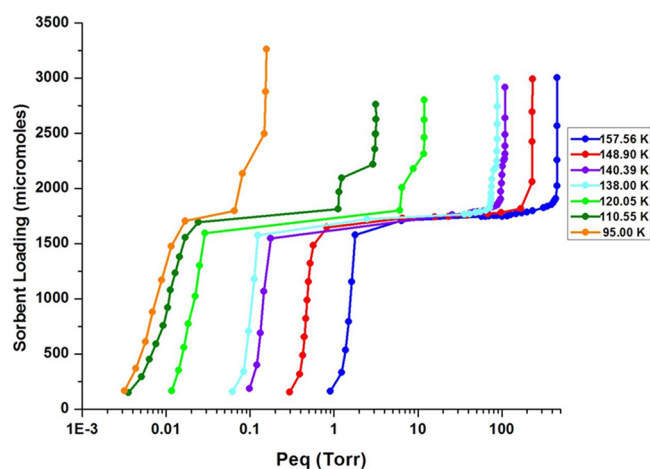


Figure 2. Adsorption isotherms for xenon in ZIF-8 at temperatures below the bulk triple point. The sorbent loading is displayed on the Y axis, and the pressure (in Torr) is presented in a logarithmic scale on the X axis. The solid curves are guides to the eyes.

for all the isotherms shows at least two prominent substeps (i.e., quasi-vertical or sharply steeped segments) in the adsorption data. The substep present at the highest loadings and pressures for each temperature corresponds to saturation being reached. At the saturated vapor pressure, the loading increases without any further increase in pressure. In this region, bulk solid Xe is forming on the sorbent and in the sample cell. We used the value of the saturated vapor pressure,

together with Antoine's equation, to determine the isotherm temperatures (i.e., we cross-calibrated the sample cell thermometer against xenon's sublimation pressure).²⁹

The second substep present in all the isotherms is the largest one in terms of loading interval below saturation. It is present at low pressures for each temperature. This substep corresponds to the sorption of xenon atoms on the most attractive sites available for them in the ZIF-8. These are the sites that have been identified as being the most numerous in the synchrotron X-ray diffraction study of Xe on ZIF-8, and correspond to Xe adsorbing near the imidazole ligands.²³

In addition to these two substeps, isotherms measured below 148 K display an additional substep at pressures and loadings intermediate between those of the low-pressure substep and saturation. This additional step corresponds to the "gate-opening" transition of the ZIF-8.^{14–18} As a result of the reorientation of the imidazole linkers which takes place in gate-opening, the size of the windows to the center of the cage increases, thus making available the sites at the center of the pore for xenon sorption, as was described in the Introduction.²³ The isotherm results displayed in Figure 2 are the first ones to show the presence of the gate-opening substep for Xe sorption on ZIF-8.

As Figure 2 shows, the substep indicative of the transition is sharper at lower temperatures. It is clear from the same figure that the gate-opening transition occurs increasingly closer to the saturated vapor pressure as the isotherm temperatures increase. Substeps in adsorption isotherms indicative of the gate-opening transition have been reported for isotherms of other gases on N_2 , O_2 , CO , and Ar in ZIF-8.^{14–18}

3.2. Isostatic Heat of Adsorption. We have determined the isosteric heat of adsorption as a function of sorbent loading from the adsorption isotherm data using the relation^{30,31}

$$q_{st} = k_B T^2 \left(\frac{\partial \ln P}{\partial T} \right)_n \quad (1)$$

here q_{st} is the isosteric heat of adsorption, k_B is Boltzmann's constant, P is the equilibrium pressure, T is the temperature, and n is the value of the sorbate loading at which the isosteric heat is being obtained. Assuming that the xenon in the gas

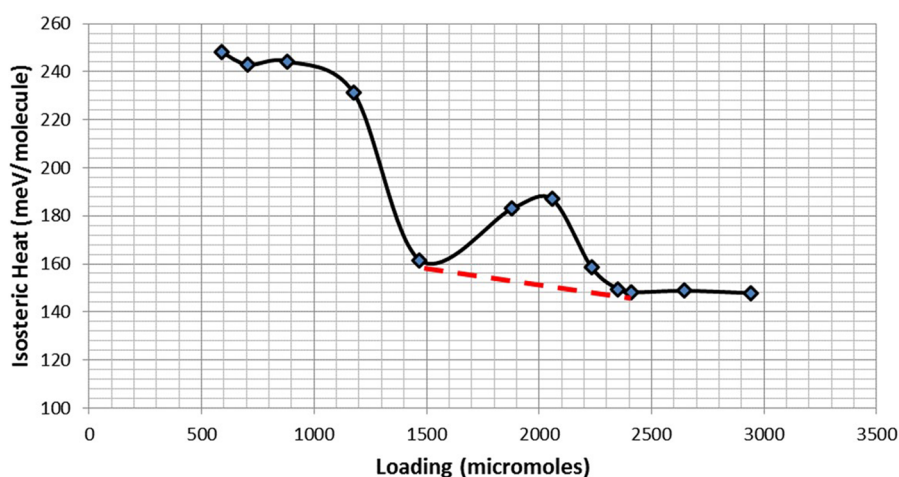


Figure 3. Isostatic heat of adsorption plotted as a function of sorbent loading for xenon in ZIF-8. The low-loading value corresponds to sorption in the high-binding energy sites on the ZIF-8. The local maximum, near 2000 μmol , corresponds to the gate-opening substep. The height of the peak associated with gate-opening, relative to a linear background, is approximately 36 meV. The value of the isosteric heat at loadings above 2500 μmol is the heat of sublimation for Xe. (The curve is a guide to the eyes.)

phase behaves like an ideal gas, this equation yields solutions of the general form

$$\ln P_n = -\frac{(q_{st})_n}{k_B T} + b \quad (2)$$

where P_n is the pressure at a given value of the sorbent loading, n , for temperature T .

If, for a given loading n , $\ln(P_n)$ is plotted as a function of the inverse of the isotherm temperature, the slope of the resulting straight line yields the isosteric heat of adsorption for that loading. Thus, the isotherm data allows the determination of the isosteric heat of adsorption as a function of loading.

When the system reaches saturation, substituting $\ln P_{\text{sat}}$ for $\ln P_n$, and making use of the Clausius–Clapeyron equation allows the determination of the value for the latent heat of sublimation for xenon (over the range of temperatures studied, the bulk phase is the solid). Comparing the value of the latent heat of sublimation obtained from our isotherm measurements with values for the bulk heat of sublimation reported in the literature provides an internal test of the accuracy of our isosteric heat determination.

The loading dependence of the isosteric heat of adsorption is shown in Figure 3.

The isosteric heats of adsorption shown in Figure 3 were calculated as follows: for the first near-horizontal segment (loadings below 1200 μmol), the isosteric heat corresponds to the values for adsorption on the high energy binding sites, that is, the low-pressure substep in the adsorption isotherm. The steep decrease in isosteric heat values near loadings of 1500 μmol corresponds in the isotherms to the rapid increase in pressure with loading present after the low pressure substep is completed. The local maximum, or peak, in the isosteric heat present near 2000 μmol corresponds to the substep resulting from the gate-opening transition region in the isotherms of Figure 2 (data corresponding to this isosteric heat peak were calculated using only those isotherms displaying the extra substep). Finally, the horizontal portion at high loadings (2400 μmol and above) corresponds to the isosteric heat at the saturated vapor pressure.

The result for the isosteric heat at the saturated vapor pressure (obtained averaging the values at the four highest loadings in Table 1) is 148.6 meV. This value corresponds very well with the reported latent heat of sublimation for xenon (of 150 meV).²⁹

We can use the data in Figure 3 to obtain an estimate for an upper bound for the heat of transformation involved in the gate-opening transition. We note that there are, in fact, two transitions associated with gate-opening: the gate-opening transition in the ZIF-8 itself and the transition from the gas phase to the sorbed phase taking place in the newly available sites that become available in the ZIF-8 as a result of gate-opening. We make the assumption that the value of the heat of transition determined from the isotherm data in the gate-opening substep is the sum of two terms: the heat of adsorption in the available sites and the heat associated with the structural transition in the ZIF-8. If we were to assume that the isosteric heat peak were due solely to gate-opening, we would obtain a value of ~ 36 meV for the upper bound value for the heat of transition of ZIF-8. (We note that the heat of transition will necessarily be smaller than this upper bound, because a sizable contribution to the isosteric heat peak comes from the sorption

Table 1. Isosteric Heat of Adsorption as a Function of Sorbent Loading^a

loading (μmol)	isosteric heat (meV/molecule)
587.8	248.2
705.4	243.0
881.8	244.3
1175.7	231.1
1469.6	161.0
1881.1	183.1
2057.5	188.0
2233.8	158.3
2351.4	149.5
2410.2	148.2
2645.3	148.8
2939.2	148.0

^aData presented corresponds to that in Figure 3.

of Xe on the new sites that become available in the ZIF-8 as a result of gate-opening.)

Recently,¹⁸ we have reported on O_2 sorption in ZIF-8. O_2 in ZIF-8 is another system that exhibits the gate-opening transition. Following a different reasoning from the one described above, we obtained an estimate of about 30 meV for the upper bound of the heat associated with the gate-opening transition in the case of O_2 sorption on ZIF-8.¹⁸ In light of the rather crude approximations made in arriving at both of these estimates of the upper bound for the heat of transition, the agreement in the values obtained is surprisingly good.

3.3. Computer Simulations. Monte Carlo simulations were conducted for Xe in ZIF-8. The interactions were described using a pairwise Lennard-Jones potential. Several force fields have been used in the literature to study gas sorption in ZIF-8. Fairen-Jimenez et al. used the UFF force field¹⁴ to study N_2 , and modified UFF(*) and UFF(+) parameters to study CH_4 , C_2H_6 , and CO_2 .²⁴ The Dreiding force field was used by Snurr's group to study xenon–krypton mixtures²⁵ and by Wu et al. to study ethane–ethylene mixtures.²⁶

Here we have used a new force field that is a mixture between the UFF(*) and the Dreiding parameters, which we call the mixed force field (or MFF). We explain the need to develop this new set of parameters in what follows.

The LJ parameters for the sorbent are listed in Table 2. The potential energy of interaction between two fluid particles is calculated using the Lennard-Jones 12-6 equation

$$\phi_{\text{ff}}(r) = 4\epsilon_{\text{ff}} \left[\left(\frac{\sigma_{\text{ff}}}{r} \right)^{12} - \left(\frac{\sigma_{\text{ff}}}{r} \right)^6 \right] \quad (3)$$

where r is the separation between the two particles.

The interaction energy between a fluid particle and a ZIF-8 atom is also calculated by eq 3 with σ_{ff} and ϵ_{ff} replaced by σ_{sf} and ϵ_{sf} , respectively (with sorbate–sorbent parameters obtained using the Lorentz–Berthelot mixing rules).³¹

The total energy is calculated by summing the pairwise interactions between fluid particles and between individual atoms and fluid particles as follows:

$$U = \sum_{i,j>i} \phi_{ij}(r_i - r_j) + \sum_{i,k} \phi_{ik}(r_i - r_k) \quad (4)$$

Table 2. Lennard-Jones Interaction Parameters Used for the Simulations

	Dreiding		UFF		UFF(*)		UFF(+)		MFF	
	ϵ_{xx}/k_B	$\sigma_{xx}/\text{\AA}$	ϵ_{xx}/k_B	$\sigma_{xx}/\text{\AA}$	ϵ_{xx}/k_B	$\sigma_{xx}/\text{\AA}$	ϵ_{xx}/k_B	$\sigma_{xx}/\text{\AA}$	ϵ_{xx}/k_B	$\sigma_{xx}/\text{\AA}$
C	47.890	3.47	52.838	3.431	33.288	3.063	31.270	3.431	47.890	3.063
H	7.650	2.85	22.142	2.571	13.949	2.276	13.103	2.571	7.650	2.276
Zn	27.700	4.04	62.399	2.462	39.312	2.198	36.928	2.462	27.700	2.198
N	38.980	3.26	34.722	3.261	21.875	2.911	20.549	3.261	38.980	2.911

Here, r_i and r_j are the positions of fluid particles i and j , respectively; r_k is that of a carbon atom; ϕ_{ij} is the pair interaction potential energy between fluid particles; and ϕ_{ik} is that between particle i and carbon atom k .

The heat of adsorption ΔH° is the difference between the molar enthalpy of the sorbate in the vapor phase and the partial molar enthalpy of the sorbed phase. Assuming that the molar kinetic energy is the same in the gas and in the sorbed state, the heat of adsorption can be expressed as a function of the total molar potential energy in the vapor phase, E_t^g , and that in the sorbed phase E_t^s .

$$-\Delta H^\circ = RT - E_t^s - E_t^g \quad (5)$$

In GCMC simulations, it is equivalent to calculate $-\Delta H^\circ$ using the method outlined above or to use the partial derivatives of the average total energy with respect to the average number $\langle N \rangle$ of adsorbed molecules:

$$\Delta H^\circ = RT - \frac{\partial \langle E_t^s \rangle}{\partial \langle N \rangle} + \frac{\partial \langle E_t^g \rangle}{\partial \langle N \rangle} \quad (6)$$

The isosteric heat of adsorption Q_{st} can, thus, be calculated by the fluctuations method

$$Q_{st} = RT - \left\{ \frac{[\langle E_t N \rangle - \langle E_t \rangle \langle N \rangle]}{[\langle N^2 \rangle - \langle N \rangle^2]} \right\} \quad (7)$$

where E_t is the sum of two terms: the potential energy between adsorbed molecules and the adsorbent surface.

A central goal of our simulations of sorption on ZIF-8 is to obtain the values of the isosteric heat of adsorption for the system before and after the gate-opening transition. For computational simplicity, rather than conducting simulations that include explicitly the flexibility of the ZIF-8, we have opted to simulate Xe sorption on the known structures before (the AP, or as-produced, structure) and after (the HP, or high-pressure, structure) the gate-opening transition, and to compare the results obtained from the simulations with those from the experiments. (The AP and HP structures were generated on the basis of the crystallographic data for the ZIF-8 system.¹⁹ The simulation cells were obtained using the OLEX2 software.³²) As has been noted (and explained in some detail) before,³³ even when the simulations include the flexibility of ZIF-8, what is used is a hybrid (grand-canonical Monte Carlo–molecular dynamics) approach. Sorption is simulated using GCMC on a rigid ZIF-8 structure for a given pressure. Then, to relax the rigid ZIF-8 structure, MD simulations are performed at the fixed pressure, and new structural parameters are obtained. These new parameters are used in a subsequent GCMC simulation on a rigid structure, and the process is repeated until the MD does not produce new relaxed values. Our approach does not reproduce the transition in the ZIF-8 but allows for the computation of the isosteric heat for the correct structures below and above the transition. These are results that we compare to the experiments.

The simulation cells for the adsorption isotherms were cubic cells; each cubic simulation cell contains 8 ($2 \times 2 \times 2$) unit cells of ZIF-8. The lattice parameters for the \AA unit cells are, for the AP structure, $a = b = c = 16.9920 \text{\AA}$, so the simulation cell has the dimensions $33.984 \times 33.984 \times 33.984$ and, for the HP structure, $a = b = c = 17.0710 \text{\AA}$, so the simulation cell has the dimensions $34.142 \times 34.142 \times 34.142$ both with periodic boundary conditions in X , Y , and Z .^{17,34} As a result of the boundary conditions chosen, the simulated system is effectively infinite, and neither adsorption on the surface of the ZIF-8 nor saturation can occur in the simulations. The results of the computer simulations for the adsorption isotherms for both the AP well as the HP structures, obtained with the different sets of parameters listed in Table 2, are presented in Figure 4.

A different simulation cell was used for the isosteric heat. The dimensions of the cell were $33.984 \times 33.984 \times 84.96$ for the AP and $34.142 \times 34.142 \times 85.355$ for the HP structure with also 8 ($2 \times 2 \times 2$) unit cells of ZIF-8 in the bottom, in order to allow Xe atoms to explore the surface of the MOF and not only the interior, with periodic boundary conditions in X and Y and a

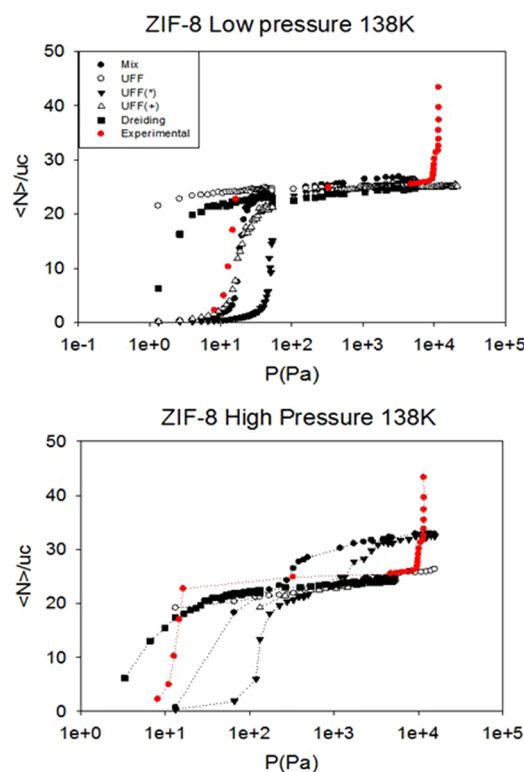


Figure 4. Upper panel: simulation for the 138 K isotherm in the lower pressure (AP) structure, i.e., before the gate-opening transition. Lower panel: simulation on the structure after gate-opening (HP structure). The red full circles are experimental data. The isotherms for the two structures, AP and HP, are calculated using the various sets of parameters listed in the legend (which applies to both panels).

reflecting plane in Z . The simulation results are expressed in terms of the number of atoms/unit cell.

In the upper panel, it can be seen that, for the AP structure, the simulation results with the UFF(+) force field (open triangles) agree very well with the experimental data. The relevant portion for determining where the AP structure correctly describes the sorbent is for loadings below approximately $\langle N \rangle / uc = 20$.

However, the agreement obtained using the UFF(+) set of parameters for the HP structure is not good; see lower panel. The resulting isotherm is not able to capture the increase in the number of adsorbed Xe atoms in the HP structure (here the relevant portion for comparison with the experiments is for $\langle N \rangle / uc$ above 20).

We note that similar behavior is obtained using the UFF, Dreiding, and UFF(+) force fields. None of them yield the experimentally observed loading increase for the HP structure. The fact that UFF(+) and UFF have the same σ Lennard-Jones parameters and both have the same problem suggests that these parameters are not optimized for the sorption of large sorbents such as xenon.

As shown in the lower panel of Figure 4, the isotherm calculated with the UFF(*) parameters (inverted full triangles) shows the correct increase in loading for the HP ZIF-8 structure. However, these parameters yield an isotherm in the AP structure that considerably overestimates the sorption pressure.

These observations led us to keep the σ parameters of the UFF (*) and to increase the ϵ parameter. The best fit to the isotherms was found using the Dreiding ϵ parameters and UFF(*) σ parameters. This is the set that we have called MFF in Table 2. The MFF produces good results with the AP ZIF-8 structure, and it also provides the increase in loading that accompanies the structural transformation to the HP structure. Figure 5 shows the result of our simulation using the AP structure and our optimized parameters.

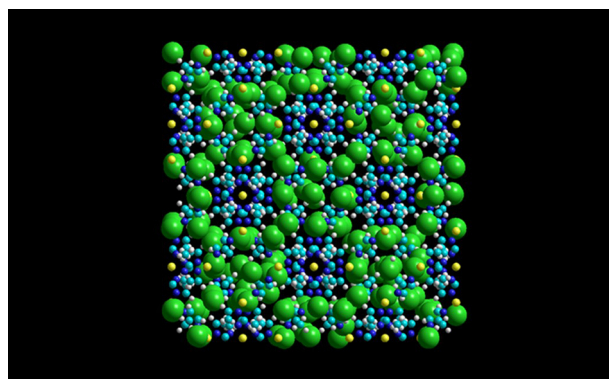


Figure 5. Xenon conformations on ZIF-8 AP. Xenon atoms are in green. ZIF-8 atoms are not drawn to scale for the sake of clarity. N atoms are in blue, C atoms are in cyan, Zn atoms are in yellow, and H atoms are in white. It can be seen that Xe atoms form a hexagonal arrangement.

As is shown in the Supporting Information, the MFF accounts well for the data over the entire range of the temperatures studied.

The transferability of this newly developed potential was checked by performing simulations of methane and argon adsorption. The results that we have obtained are in excellent

agreement with the isotherms obtained by Fairen-Gimenez et al.²⁴ for methane at 125 K and Pantatosaki³⁵ for argon at 87 K. This allows us to conclude that the MFF is an excellent set of parameters for simulating adsorption on ZIF-8.

Our simulation results for the isosteric heat of adsorption are shown in Figure 6. We note that, while Figure 6 shows results

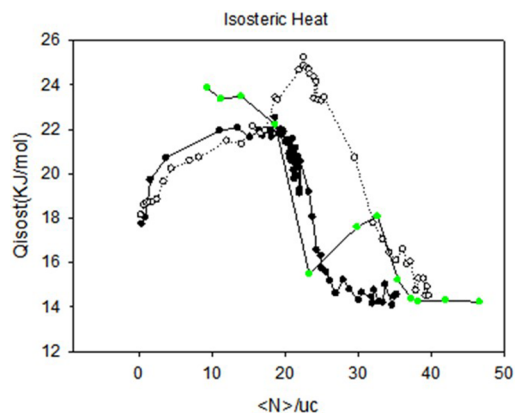


Figure 6. Isosteric heat of adsorption. Black full circles, ZIF-8 AP; black empty circles, ZIF-8 HP; green full circles, experimental isosteric heat.

for both ZIF-8 structures at all loadings, the AP structure corresponds to the experimentally measured values at the lower loadings and the HP structure at higher loadings (see Figure 3).

Figure 6 shows that at low loadings there are no significant differences in the sites of adsorption, with values for the ZIF-8 HP structure being somewhat lower than those obtained from the ZIF-8 AP structure. We note that these isosteric heat values at low loadings are below the region that was studied experimentally.

While the simulations are not able to reproduce the experimentally high value that we found at relatively low loadings (of 24 kJ/mol) in the experiments, there is otherwise very good agreement between experiment and simulations with the isosteric heat calculated from the AP structure at lower loadings and with the HP structure and experiments at high loadings (above about 34 in the scale of Figure 6). The isosteric heat peak observed in the experiments can be understood, to a great extent, from the simulations as corresponding to the difference in adsorption energies, for the same loading, between the sites available in the AP and the HP structures.

The last few experimental points, which correspond to the formation of bulk, have no correspondence in the simulations, as we have discussed previously.

We have explored the kinetics of adsorption for Xe in ZIF-8. We did this by measuring the approach to equilibrium of the loading of the ZIF-8 sample after a dose of xenon is added to the sample cell (i.e., by measuring sample loading vs time after a dose of xenon is added to the cell). In our measurements, the ZIF-8 already contains whatever amount of Xe had been added before the new dose is admitted into the sample cell: the measurements of approach to equilibrium as a function of time are carried out for each point along each isotherm.

The approach to equilibrium data is presented in Figure 7. Plotted in this graph is the fractional pressure distance to equilibrium in the sample cell after a time t has elapsed, $[(P(t) - P_{eq})/P_{eq}]$, as a function of the elapsed time (here $P(t)$ is the pressure in the cell at time t after gas was added to it, and P_{eq} is

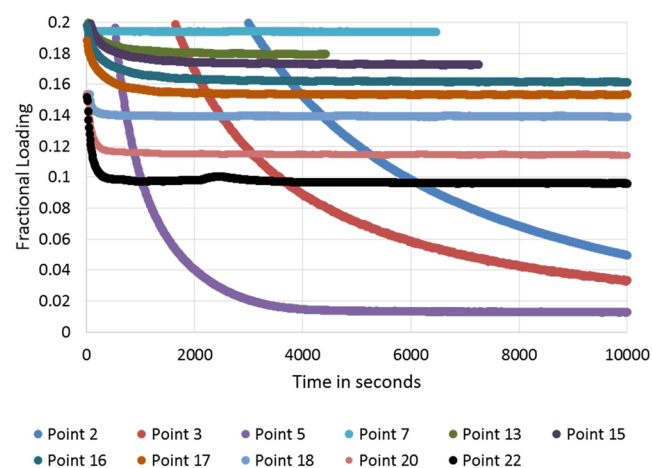


Figure 7. Approach to equilibrium for points along the 138 K isotherm.

the value of the equilibrium pressure for that loading).¹⁷ The equilibration data is presented for various points along the 138 K, including along the gate-opening substep region. The number associated with each curve is the order of that point in the isotherm (i.e., the first point measured in the isotherm, at the lowest equilibrium loading, is curve #1; the second point measured, at the second-lowest loading, is curve #2, etc.). In Figure 7, the system reaching equilibrium corresponds to the fractional distance to equilibrium curves becoming parallel to the horizontal time elapsed axis. (In Figure 7, the curves have been shifted vertically for the sake of clarity; otherwise, all of the features of interest would collapse and overlap on the horizontal axis.)

Curves #2 and #3 correspond to measurements conducted during adsorption in the highest energy binding sites. Curve #5 is at the end of this higher binding site region, and curve #7 corresponds to a point in the nearly horizontal region that exists between the higher binding energy sites and the gate-opening substep. For all the curves in the range from #2 to #7, the equilibration time is a decreasing function of the loading.

We note that the first two points in this region, #2 and #3, have not yet reached equilibrium even after more than 10,000 s have elapsed since the time at which the gas was dosed into the cell. It is apparent from the data shown in the figure that equilibration is slower the lower the equilibrium loading.

This dependence of equilibration time on coverage reverses after curve #7. For data points corresponding to sorption in the space that becomes available as a result of the structural transition in ZIF-8 (curves #13–17), reaching equilibrium requires a longer time than in the region just preceding it (at lower equilibrium loadings). We note that significant times are required to reach equilibrium in this gate-opening region, as well: for loadings in this region, more than 2000 s have to elapse before equilibrium is reached.

Once this additional space is filled, condensation is rapidly reached. Again, there is a reversal, as the time required for equilibration in this region (curves #18–22) is shorter than that in the gate-opening region. We had observed similar behavior with O₂ in ZIF-8.¹⁸

4. DISCUSSION

Our experimental result, that the substep corresponding to the gate-opening transition stops appearing as a distinct feature in

the isotherms at temperatures above 145 K, is consistent with the result of the ¹²⁹Xe NMR study,²¹ which found evidence of a large chemical shift in the range between 150 and 170 K. Those authors stated that the shift may be indicative of the imidazolate linkers undergoing reorientation (i.e., gate-opening).

We note that at the two highest temperatures at which we have conducted measurements the isotherms do not abruptly and sharply intersect the vertical line corresponding to the saturated vapor pressure, contrary to the behavior observed at lower temperatures where saturation is reached abruptly. For these two temperatures, the adsorption curve approaches the saturated vapor pressure in a more gradual manner with increasing loading as the pressure gradually increases to saturation. This suggests that the fact that there is not a sharp step in the isotherms is not an indication that no further adsorption is occurring: adsorption still is occurring, but it is taking place more gradually than at a sharp gate-opening transition. This last observation is consistent with the results reported in the synchrotron diffraction study of xenon on ZIF-8 which reports, for a temperature of 180 K, the gate-opening phenomenon starts occurring at a relative pressure somewhere between $P/P_0 = 0.042$ and $P/P_0 = 0.179$.²³ The occupation of these additional sites in that study appears to be much more gradual than the one we have observed at lower temperatures. In the synchrotron study, sorption is still taking place in the stronger binding sites when the center pore sites start being occupied.²³

The structural study reports that the loading of the sites available as a result of sorption at the center of the pore (the sites available as a result of gate-opening) is 8% of the size of the loading on the strongest binding sites.²³ If we take the ratio of the loading corresponding to the gate-opening substep to the lower loading/lower pressure substep to represent this same ratio in our experiments, we find for it a value of approximately 15%, which is in reasonable agreement with what is expected, given the ambiguities in our determination of this quantity.

We note that the peak or local maximum that we have found in the isosteric heat of adsorption occurs at the same loading as the substep associated with the gate-opening transition (compare the sorbent loading scales in Figures 2 and 3 in the regions corresponding to the substep and the peak, respectively). Thus, this peak in the plot of the isosteric heat of adsorption as a function of sorbent loading provides an alternative thermodynamic approach for identifying the presence of gate-opening for ZIF-8. This feature may be especially useful for those cases in which the gate-opening transition occurs, but there is no corresponding sharp feature in the adsorption isotherm.

Our results for the kinetic measurements show that, for the range of temperatures where gate-opening appears as a substep in the isotherm, the adsorption kinetics for the system is a nonmonotonic function of sorbent loading. This is a consequence of the fact that the sorbent experiences a phase transition as a function of sorbent loading, and it indicates a difference in the accessibility of the sites at the center of the pore relative to those of other sites present on this sorbent. This nonmonotonic dependence of equilibration time on sorbent loading is unusual.

We note that when both the lower loading, stronger binding sites as well as the sites at the center of the pore are taken separately, adsorption equilibrium is reached faster for higher loadings. This inverse relation between sorbent loading and

equilibration times for a given set of adsorption sites is the one expected for a spherical sorbate.³⁵

5. CONCLUSIONS

We have found that there is a substep in the adsorption isotherm data for Xe in ZIF-8 associated with the gate-opening transition for this system. While this feature had been observed for other sorbates (Ar, N₂, O₂, and CO),^{16,18} this is the first time that such a feature has been observed for xenon.

We obtained the values for the isosteric heat of adsorption in the substep corresponding to the high energy binding sites, for the substep corresponding to gate-opening, and for the bulk heat of sublimation from the isotherm data.

Our Monte Carlo computer simulations, conducted using a new set of Lennard-Jones parameters, which we termed “mixed” parameters, are able to reproduce both the features of the isotherms (before and after gate-opening) as well as the values of the isosteric heat better than other sets of parameters that had been used in previous simulation studies of sorption in ZIF-8.^{14,24–26} We verified the transferability of this potential by performing calculations for Ar and methane sorption on ZIF-8, with excellent results.

We have determined the existence of a peak in the isosteric heat of adsorption (when it is plotted as a function of sorbent loading) which corresponds to the gate-opening transition. This suggests that measuring the isosteric heat as a function of loading can be used as an alternative thermodynamic way to explore the existence of a gate-opening transition in those sorbed systems that do not show an explicit substep in the sorption data.

Since the substep corresponding to gate-opening involves both the transition that is taking place on the ZIF-8 sorbent itself as well as the transition from the gas to the adsorbed phase in the space that becomes available, by making a few reasonable simplifying assumptions, we were able to obtain an upper bound for the value for the heat of transition for gate-opening of 36 meV which is in reasonably good agreement with the value we had obtained before for this quantity for the case of O₂ sorption.¹⁸

We measured the kinetics of adsorption along the isotherms. We monitored the time required to reach equilibrium. This quantity depends nonmonotonically on the loading. The equilibration times decrease with increasing loading when adsorption is taking place on the higher binding energy sites. Then, in the region corresponding to the gate-opening substep in the isotherm, the equilibration times increase. After this region is completed, the equilibration times once again decrease with increasing loading. This loading dependence of the kinetics of adsorption exhibited by Xe on ZIF-8 is unusual; in most cases, the dependence of kinetics on loading is monotonic.

■ ASSOCIATED CONTENT

Supporting Information

The Supporting Information is available free of charge on the ACS Publications website at DOI: 10.1021/acs.jpcc.6b03481.

Additional figures for experimental and simulated isotherms (PDF)

■ AUTHOR INFORMATION

Corresponding Author

*Phone: 618-453-2044. E-mail: aldo@physics.siu.edu.

Author Contributions

The manuscript was written through contributions of all authors. All authors have given approval to the final version of the manuscript.

Notes

The authors declare no competing financial interest.

■ ACKNOWLEDGMENTS

The authors gratefully acknowledge financial support granted via a joint collaboration project of CONICET (Argentina) and NSF (USA). A.G.A. also thanks UnCaFiQT (SNCAD) for computational resources. A.G.A. is a CONICET fellow.

■ REFERENCES

- (1) Yang, R. T. *Adsorbents: Fundamentals and Applications*; John Wiley & Sons: Hoboken, New Jersey, USA, 2003.
- (2) Serre, C.; Millange, F.; Thouvenot, C.; Noguès, M.; Marsolier, G.; Louër, D.; Férey, G. Very Large Breathing Effect in the First Nanoporous Chromium (Iii)-Based Solids: Mil-53 or Criii (Oh)O{O2c-C6h4-Co2}O{Ho2c-C6h4-Co2h} XO H2o Y. *J. Am. Chem. Soc.* **2002**, *124*, 13519–13526.
- (3) Férey, G.; Serre, C. Large Breathing Effects in Three-Dimensional Porous Hybrid Matter: Facts, Analyses, Rules and Consequences. *Chem. Soc. Rev.* **2009**, *38*, 1380–1399.
- (4) Kitagawa, S.; Kitaura, R.; Noro, S. i. Functional Porous Coordination Polymers. *Angew. Chem., Int. Ed.* **2004**, *43*, 2334–2375.
- (5) O’Keeffe, M.; Yaghi, O. M. Deconstructing the Crystal Structures of Metal–Organic Frameworks and Related Materials into Their Underlying Nets. *Chem. Rev.* **2012**, *112*, 675–702.
- (6) Juan-Alcañiz, J.; Gascon, J.; Kapteijn, F. Metal–Organic Frameworks as Scaffolds for the Encapsulation of Active Species: State of the Art and Future Perspectives. *J. Mater. Chem.* **2012**, *22*, 10102–10118.
- (7) Li, J.-R.; Sculley, J.; Zhou, H.-C. Metal–Organic Frameworks for Separations. *Chem. Rev.* **2012**, *112*, 869–932.
- (8) Sing, K. S. Reporting Physisorption Data for Gas/Solid Systems with Special Reference to the Determination of Surface Area and Porosity (Recommendations 1984). *Pure Appl. Chem.* **1985**, *57*, 603–619.
- (9) Huang, X. C.; Lin, Y. Y.; Zhang, J. P.; Chen, X. M. Ligand-Directed Strategy for Zeolite-Type Metal–Organic Frameworks: Zinc (Ii) Imidazolates with Unusual Zeolitic Topologies. *Angew. Chem.* **2006**, *118*, 1587–1589.
- (10) Park, K. S.; Ni, Z.; Côté, A. P.; Choi, J. Y.; Huang, R.; Uribe-Romo, F. J.; Chae, H. K.; O’Keeffe, M.; Yaghi, O. M. Exceptional Chemical and Thermal Stability of Zeolitic Imidazolate Frameworks. *Proc. Natl. Acad. Sci. U. S. A.* **2006**, *103*, 10186–10191.
- (11) Hayashi, H.; Cote, A. P.; Furukawa, H.; O’Keeffe, M.; Yaghi, O. M. Zeolite a Imidazolate Frameworks. *Nat. Mater.* **2007**, *6*, 501–506.
- (12) Sold by Sigma-Aldrich as Basolite Z1200, manufactured by BASF.
- (13) Chmelik, C. Characteristic Features of Molecular Transport in Mof Zif-8 as Revealed by Ir Microimaging. *Microporous Mesoporous Mater.* **2015**, *216*, 138–145.
- (14) Fairen-Jimenez, D.; Moggach, S.; Wharmby, M.; Wright, P.; Parsons, S.; Duren, T. Opening the Gate: Framework Flexibility in Zif-8 Explored by Experiments and Simulations. *J. Am. Chem. Soc.* **2011**, *133*, 8900–8902.
- (15) Kapko, V.; Dawson, C.; Treacy, M.; Thorpe, M. Flexibility of Ideal Zeolite Frameworks. *Phys. Chem. Chem. Phys.* **2010**, *12*, 8531–8541.
- (16) Ania, C. O.; García-Pérez, E.; Haro, M.; Gutiérrez-Sevillano, J.; Valdés-Solís, T.; Parra, J.; Calero, S. Understanding Gas-Induced Structural Deformation of Zif-8. *J. Phys. Chem. Lett.* **2012**, *3*, 1159–1164.
- (17) Tanaka, H.; Ohsaki, S.; Hiraide, S.; Yamamoto, D.; Watanabe, S.; Miyahara, M. T. Adsorption-Induced Structural Transition of Zif-8:

A Combined Experimental and Simulation Study. *J. Phys. Chem. C* **2014**, *118*, 8445–8454.

(18) Russell, B.; Villaroel, J.; Sapag, K.; Migone, A. D. O₂ Adsorption on Zif-8: Temperature Dependence of the Gate-Opening Transition. *J. Phys. Chem. C* **2014**, *118*, 28603–28608.

(19) Moggach, S. A.; Bennett, T. D.; Cheetham, A. K. The Effect of Pressure on Zif-8: Increasing Pore Size with Pressure and the Formation of a High-Pressure Phase at 1.47 GPa. *Angew. Chem.* **2009**, *121*, 7221–7223.

(20) Soleimani Dorcheh, A.; Denysenko, D.; Volkmer, D.; Donner, W.; Hirscher, M. Noble Gases and Microporous Frameworks; from Interaction to Application. *Microporous Mesoporous Mater.* **2012**, *162*, 64–68.

(21) Springuel-Huet, M.-A.; Nossov, A.; Guenneau, F.; Gédéon, A. Flexibility of Zif-8 Materials Studied Using ¹²⁹Xe Nmr. *Chem. Commun.* **2013**, *49*, 7403–7405.

(22) Ryan, P. J.; Farha, O. K.; Broadbelt, L. J.; Snurr, R. Q.; Bae, Y.-s. Metal-Organic Frameworks for Xe/Kr Separation. US Patent 8,784,536, 2014.

(23) Magdysyuk, O.; Adams, F.; Liermann, H.-P.; Spanopoulos, I.; Trikalitis, P.; Hirscher, M.; Morris, R.; Duncan, M.; McCormick, L.; Dinnebier, R. Understanding the Adsorption Mechanism of Noble Gases Kr and Xe in Cpo-27-Ni, Cpo-27-Mg, and Zif-8. *Phys. Chem. Chem. Phys.* **2014**, *16*, 23908–23914.

(24) Fairen-Jimenez, D.; Galvelis, R.; Torrisi, A.; Gellan, A. D.; Wharmby, M. T.; Wright, P. A.; Mellot-Draznieks, C.; Dueren, T. Flexibility and Swing Effect on the Adsorption of Energy-Related Gases on Zif-8: Combined Experimental and Simulation Study. *Dalton Transactions* **2012**, *41*, 10752–10762.

(25) Ryan, P.; Farha, O. K.; Broadbelt, L. J.; Snurr, R. Q. Computational Screening of Metal-Organic Frameworks for Xenon/Krypton Separation. *AIChE J.* **2011**, *57*, 1759–1766.

(26) Wu, Y.; Chen, H.; Liu, D.; Qian, Y.; Xi, H. Adsorption and Separation of Ethane/Ethylene on Zifs with Various Topologies: Combining Gcmc Simulation with the Ideal Adsorbed Solution Theory (Iast). *Chem. Eng. Sci.* **2015**, *124*, 144–153.

(27) Emmett, P. H.; Brunauer, S. The Use of Low Temperature Van Der Waals Adsorption Isotherms in Determining the Surface Area of Iron Synthetic Ammonia Catalysts. *J. Am. Chem. Soc.* **1937**, *59*, 1553–1564.

(28) Kemp, R.; Kemp, W.; Smart, P. The Triple Point of Xenon as a Possible Defining Point on an International Temperature Scale. *Metrologia* **1985**, *21*, 43.

(29) Pollack, G. L. The Solid State of Rare Gases. *Rev. Mod. Phys.* **1964**, *36*, 748.

(30) Dash, J. *Films on Solid Surfaces*; Academic Press: New York, 1975.

(31) Bruch, L. W.; Cole, M. W.; Zaremba, E. *Physical Adsorption: Forces and Phenomena*; Oxford Science Publications: New York, USA, 1997.

(32) Dolomanov, O. V.; Bourhis, L. J.; Gildea, R. J.; Howard, J. A.; Puschmann, H. Olex2: A Complete Structure Solution, Refinement and Analysis Program. *J. Appl. Crystallogr.* **2009**, *42*, 339–341.

(33) Zhang, L.; Hu, Z.; Jiang, J. Sorption-Induced Structural Transition of Zeolitic Imidazolate Framework-8: A Hybrid Molecular Simulation Study. *J. Am. Chem. Soc.* **2013**, *135*, 3722–3728.

(34) Parkes, M. V.; Demir, H.; Teich-McGoldrick, S. L.; Sholl, D. S.; Greathouse, J. A.; Allendorf, M. D. Molecular Dynamics Simulation of Framework Flexibility Effects on Noble Gas Diffusion in Hkust-1 and Zif-8. *Microporous Mesoporous Mater.* **2014**, *194*, 190–199.

(35) Pantatosaki, E.; Pazzona, F. G.; Megariotis, G.; Papadopoulos, G. K. Atomistic Simulation Studies on the Dynamics and Thermodynamics of Nonpolar Molecules within the Zeolite Imidazolate Framework-8. *J. Phys. Chem. B* **2010**, *114*, 2493–2503.